Multistep direct processes in nucleon induced reactions at incident energies below 40 MeV

A. Marcinkowski[a], P. Demetriou[b], B. Mariański[a]

[a] *The Andrzej Soltan Institute for Nuclear Studies, 00-681 Warsaw, Hoża 69, Poland,*
[b] *Institute of Nuclear Physics, NCSR "Demokritos", GR-15310 Athens, Greece*

The contributions of multistep direct (MSD) reactions with different sequences of collisions of the leading continuum nucleon are presented for neutron scattering by niobium at the incident energy of 26 MeV, for the charge-exchange (p,n) reaction on copper at 27 MeV, and for proton scattering by iron at energy of 39 MeV. The MSD cross sections are calculated within the framework of the theory of Feshbach, Kerman and Koonin using the enhanced-DWBA matrix elements. The one-step cross sections allow for the excitation of the incoherent particle-hole states and of the coherent collective vibrations. The results show that in the case of neutron scattering, the dominant MSD sequence includes only reaction stages involving neutrons, while sequences including protons can be neglected. However, in the case of proton scattering and charge-exchange reactions, many of the mixed sequences including proton-proton (pp), neutron-proton (np), proton-neutron (pn) and neutron-neutron (nn) reaction stages give significant contributions to the calculated cross sections of the MSD reactions.

1 Introduction

The nucleon induced reactions to the continuum have been widely described in the framework of the theory of Feshbach, Kerman and Koonin (FKK) [1]. Following the argumentation of Feshbach [2,3], normal DWBA matrix elements were used for the description of the direct reactions. However, this resulted in negligibly small multistep direct (MSD) contributions. Thus, only the one-step direct (1SD) cross sections were used to fit the experimental data and this was possible at the expense of using different parameterizations. On the other hand, Tamura, Udagawa and Lenske [4] found that the microscopic DWBA form factors, averaged over a number of shell model particle-hole pairs, may be approximated by the derivative of the optical potential as used in analyses of inelastic scattering to collective states. This allows one to attach a formal strength parameter β_L to the cross sections for the incoherent excitation of particle-hole pairs of given orbital angular momentum L and energy. It was thus possible to analyse the microscopic cross sections in terms of the energy weighted sum rules (EWSR's) [5]. The restrictions imposed by the EWSR's resulted in reduced 1SD cross sections that include the collective, macroscopic DWBA term, summed over multipolarities $\lambda \leq 4$ and the incoherent microscopic DWBA term, summed over transferred orbital angular momenta $L > 4$ [6]. It was also shown that the reduction of the 1SD cross section could be compensated by using the enhanced non-DWBA matrix elements [7–9] originally included in the theory of FKK [1]. Furthermore it has been shown that the MSD reaction may proceed via more than one sequence of the M successive collisions of the leading continuum nucleons and the bound nucleons of the target [9,10]. In this work the different sequences that contribute to the MSD cross sections for neutron scattering, proton scattering and the charge-exchange (p,n) reaction are compared. The results show that some of the sequences are dominant whereas some others can be neglected.

2 The non-DWBA matrix elements and the enhanced MSD cross sections

The multistep cross section of the FKK theory is obtained by multiple folding of the one-step cross sections [1,11],

$$(\frac{\mathrm{d}^2\sigma}{\mathrm{dEd}\Omega})_{MSD} = \int \frac{m_1 E_1}{(2\pi)^2\hbar^2}\mathrm{dE_1 d}\Omega_1 \int \frac{\mathrm{m_2E_2}}{(2\pi)^2\hbar^2}\mathrm{dE_2 d}\Omega_2 \cdots \int \frac{\mathrm{m_{M-1}E_{M-1}}}{(2\pi)^2\hbar^2}\mathrm{dE_{M-1}d}\Omega_{\mathrm{M-1}}$$
$$\times \left(\frac{\mathrm{d}^2\sigma}{\mathrm{dE_M d}\Omega_{\mathrm{M}}}\right)_{\mathrm{1SD}} \cdots \left(\frac{\mathrm{d}^2\sigma}{\mathrm{dE_2 d}\Omega_2}\right)_{\mathrm{1SD}} \left(\frac{\mathrm{d}^2\sigma}{\mathrm{dE_1 d}\Omega_1}\right)_{\mathrm{1SD}} . \quad (1)$$

The indices M label the mass m, energy E and the solid angle Ω of the scattered nucleon after the M-th stage of the reaction. The successive 1SD cross sections in (1), apart from the last one, include the non-DWBA matrix elements. The latter are a result of the biorthogonality of the outgoing and incoming distorted waves. For each transfer of multipolarity λ or orbital angular momentum L, a number of partial waves ℓ_{M-1}, ℓ_{M-2} contribute to the incoming and outgoing distorted waves according to the triangle rule. The non-DWBA matrix elements can be obtained by multiplying each partial wave ℓ_{M-1} component of the incoming distorted wave in the normal DWBA matrix element by the inverse elastic matrix element ${S_{\ell_{M-1}}}^{-1}$ [12,13]. However, in the statistical theory of FKK the enhanced transition matrix elements are averaged over energy. To obtain the energy average we approximate the overall effect of the different averaged enhancing factors $<\mathrm{S}_{\ell_{M-1}}>^{-1}$, acting on the partial waves ℓ_{M-1} for a specific L, by an average enhancing factor $<\mathrm{S}_L>^{-1}$. The elastic scattering matrix element can be expressed in terms of the partial wave transmission coefficient T_L of the optical potential, by the relation, $\mathrm{S}_L{}^2=1 - T_L$ [13]. The energy averaging $<\mathrm{S}_L>^{-1}$ ensures that the average enhancement is smooth and free of any singularities that could arise at the energies of the single-particle resonances, where the T_L's approach unity. The smoothed enhancing factors $<\mathrm{S}_L>^{-1}$ are smaller than the ${\mathrm{S}_{\ell_{M-1}}}^{-1}$ ones [6] and provide convergent MSD cross sections.

Table 1
The decomposition of the MSD cross sections for the ^{93}Nb(n,n')^{93}Nb reaction at 26 MeV obtained with the non-DWBA matrix elements.

σ(1SD) (mb)	σ(2SD) (mb)	σ(3SD) (mb)
(ph) 214	(nnS^{-2},nn) 215	(nnS^{-2},nnS^{-2},nn) 96
(vib) 140	(npS^{-2},pn) 9.5	(nnS^{-2},npS^{-2},pn) 3.6
		(npS^{-2},pnS^{-2},nn) 2.4
		(npS^{-2},ppS^{-2},pn) 2.4
Total 354	224.5	104.4

The resulting overall enhancement of the MSD cross sections with respect to the normal DWBA ones is $(3.5\text{-}3.9)^{M-1}$ for the reactions studied.

Since (M-1) out of the M 1SD cross sections in Eq. (1) contain a sum of contributions from the enhanced one-phonon vibrations, (vibS^{-2})=$\Sigma_{\lambda\leq4}\sigma_\lambda$(vib)$<S_\lambda>^{-2}$, and from the 1SD excitations of the incoherent particle-hole pairs, (phS^{-2})=$\Sigma_{L>4}\sigma_L$(ph)$<S_L>^{-2}$, the resulting MSD cross sections consist of the following combinations of the two terms [7,8]:
1SD, (vib)+(ph),
2SD, (vibS^{-2},vib)+(phS^{-2},vib)+(vibS^{-2},ph)+(phS^{-2},ph),
3SD, etc.
The position of the enhancing factors S^{-2} indicates that they apply to the outgoing channel of the intermediate reaction stages. The collective, isoscalar one-phonon (vib) term includes the DWBA cross section calculated with a macroscopic form factor given by the derivative of the deformed optical potential. The strength is determined by the phenomenological deformation parameters of the low-energy collective levels. The strength parameters for the giant resonances are extracted from the EWSR's. The (ph) cross sections for incoherent excitation of the shell model particle-hole pairs are obtained with microscopic form factors using the real, effective interaction of Yukawa form and strength $V_{\pi\pi}$=12.7 MeV and $V_{\pi\nu}$=43.1 MeV [14], with an energy dependence according to [15]. The isovector (vib) cross section in case of the charge-exchange (p,n) reaction is calculated in an approximate way described in detail in [9]. However, in the present calculations the one-phonon (vib) and the (ph) components of the 1SD cross section are lumped together in order to minimize the number of terms in the different sequences of the reaction stages (nn), (np), (pp) and (pn) that result from the M collisions of the leading nucleon with nucleons of the target nucleus. Equation (1) is applied repeatedly for each possible sequence that contributes to the MSD reaction considered. The MSD sequences of the reaction stages that contribute to neutron scattering, to the charge-exchange (p,n) reaction and to proton scattering are listed in Tables 1 to 3, respectively. These Tables contain angle- and energy-integrated cross sections. The 1SD and 3SD emission spectra resulting from neutron and proton scattering are also shown in Figs. 1-4.

In Figs. 1 and 3 the contributions due to excitation of the one-phonon collective states

Table 2
The decomposition of the MSD cross sections for the ^{65}Cu(p,n)^{65}Zn reaction at 27 MeV obtained with the non-DWBA matrix elements.

σ(1SD) (mb)	σ(2SD) (mb)	σ(3SD) (mb)	σ(4SD) (mb)
(ph) 34	(pnS^{-2},nn) 28	(pnS^{-2},nnS^{-2},nn) 9.8	(pnS^{-2},nnS^{-2},nnS^{-2},nn) 3.15
(vib) 40	(ppS^{-2},pn) 10	(ppS^{-2},pnS^{-2},nn) 3.0	(ppS^{-2},pnS^{-2},nnS^{-2},nn) 0.90
		(ppS^{-2},ppS^{-2},pn) 0.6	(ppS^{-2},ppS^{-2},pnS^{-2},nn) 0.16
		(pnS^{-2},npS^{-2},pn) 0.2	(pnS^{-2},npS^{-2},pnS^{-2},nn) 0.05
			(pnS^{-2},nnS^{-2},npS^{-2},pn) 0.04
			(ppS^{-2},ppS^{-2},ppS^{-2},pn) 0.02
			(ppS^{-2},pnS^{-2},npS^{-2},pn) 0.007
			(pnS^{-2},npS^{-2},ppS^{-2},pn) 0.004
Total 74	38	13.6	4.3

Table 3
The decomposition of the MSD cross sections for the ^{54}Fe(p,p')^{54}Fe reaction at 39 MeV obtained with the non-DWBA matrix elements.

σ(1SD) (mb)	σ(2SD) (mb)	σ(3SD) (mb)	σ(4SD) (mb)
(ph) 78	(ppS^{-2},pp) 94	(ppS^{-2},ppS^{-2},pp) 37.6	(ppS^{-2},ppS^{-2},ppS^{-2},pp) 12.1
(vib) 80	(pnS^{-2},np) 37	(pnS^{-2},nnS^{-2},np) 10.8	(ppS^{-2},ppS^{-2},pnS^{-2},np) 2.98
		(ppS^{-2},pnS^{-2},np) 10.7	(ppS^{-2},pnS^{-2},nnS^{-2},np) 2.62
		(pnS^{-2},npS^{-2},pp) 8.0	(pnS^{-2},nnS^{-2},nnS^{-2},np) 2.61
			(pnS^{-2},npS^{-2},ppS^{-2},pp) 2.12
			(ppS^{-2},pnS^{-2},npS^{-2},pp) 1.65
			(pnS^{-2},nnS^{-2},npS^{-2},pp) 1.62
			(pnS^{-2},npS^{-2},pnS^{-2},np) 0.34
Total 158	131	67.1	26.0

(vib) and the incoherent particle-hole (ph) states are included in the 1SD cross sections for the neutron scattering (nn) and the proton scattering (pp) reaction stages, respectively. The wide maxima at the medium excitation energies, in Figs. 1 and 3, correspond to the giant resonances. The structure at the highest outgoing energies is due to the individual one-phonon states. The energy distribution of the collective states is Gaussian with width Γ=2 MeV that allows for the experimental energy resolution and the spread of the weak coupling multiplets. These structures survive the energy smearing due to the convolution

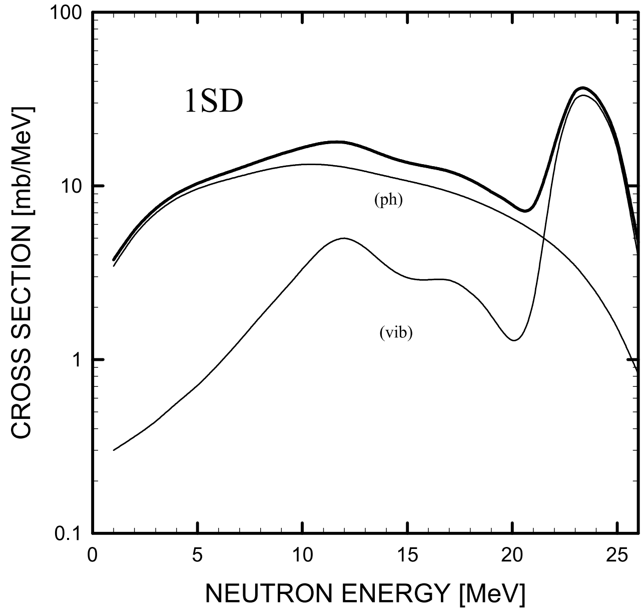

Fig. 1. The calculated 1SD neutron spectrum from the ^{93}Nb(n,n')^{93}Nb reaction, at incident neutron energy of 26 MeV (thick solid line). The contributions due to excitation of one-phonon collective states of multipolarity $\lambda \leq 4$ and to incoherent excitation of ph-pairs of transferred orbital angular momenta $L>4$ are shown separately.

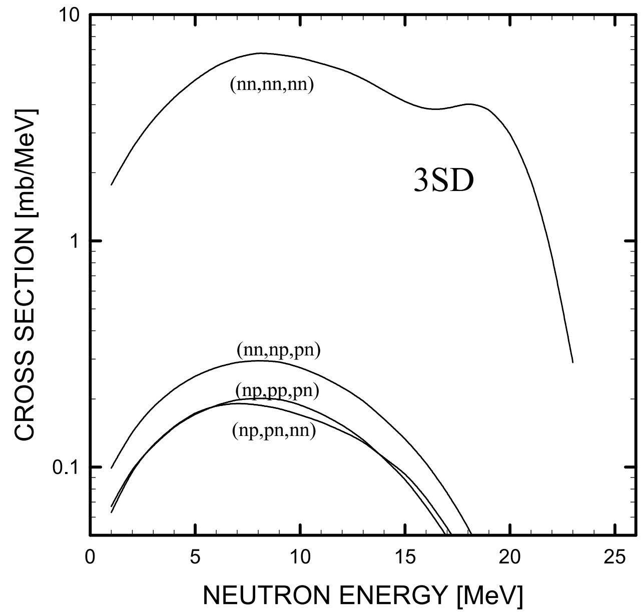

Fig. 2. The same as in Fig. 1 but for the 3SD component. The contributions from the four sequences of reaction stages are also shown as thin lines (sum of the four contributions is indistinctive from the strongest one). The enhancing factors are omitted for simplicity.

of three successive neutron scattering stages, (nnS^{-2},nnS^{-2},nn), as well as of three successive proton scattering stages, (ppS^{-2},ppS^{-2},pp), in Eq. (1), and appear, although weaker, as three-phonon structures at trice higher excitation energies in the 3SD spectra of Figs. 2 and 4. The latter figures show the emission spectra of all four sequences of reaction stages that contribute to the 3SD neutron and proton scattering, respectively.

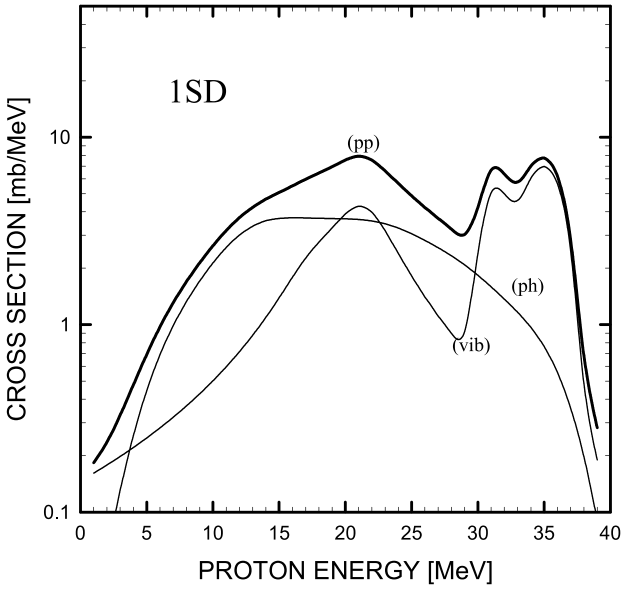

Fig. 3. The same as in Fig. 1 but from the $^{54}Fe(p,p')^{54}Fe$ reaction at incident energy of 39 MeV.

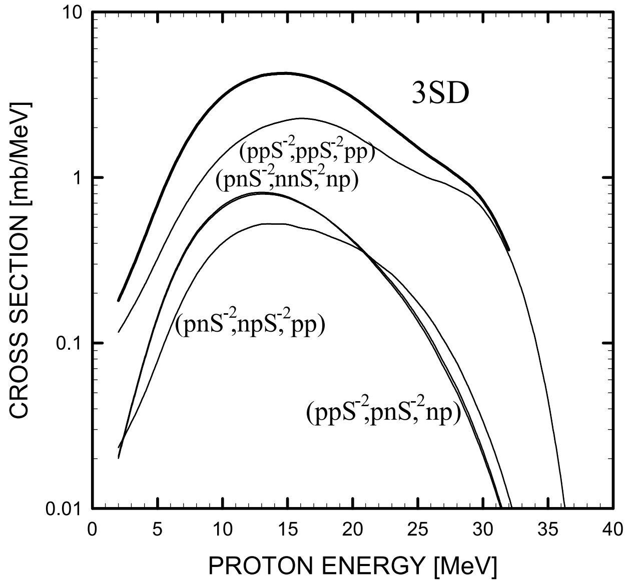

Fig. 4. The same as in Fig. 3 but for the 3SD component (thick solid line). The contributions from the four sequences of reaction stages are also shown as thin lines.

From Table 1 and Fig. 2 it is evident that the sequences of successive neutron scattering stages (nn,nn....) dominate markedly over the other ones that also involve the (np), (pn) or (pp) stages (compare also [16]). The latter sequences contribute to less than 8% of the respective MSD cross sections and therefore can be neglected. On the other hand, from Fig. 4 and Table 3 one can see that in proton scattering the sequences that also include neutrons contribute up to about 50% of the respective MSD cross sections. This

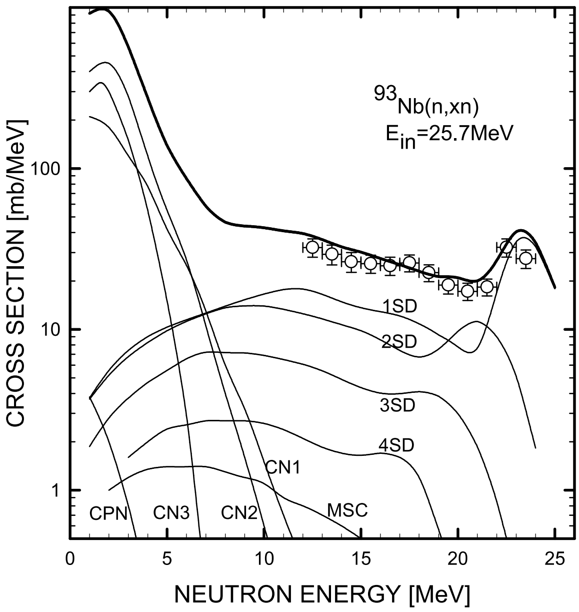

Fig. 5. Comparison of the MSD cross sections calculated with the non-DWBA matrix elements with the inclusive spectrum of neutrons emitted from the ^{93}Nb(n,xn)^{93}Nb reaction at incident energy of 26.7 MeV [17]. Labels CN1, CN2, CN3 show the primary, secondary and tertiary neutrons from the compound nucleus. CPN denotes neutrons preceded by evaporation of a proton.

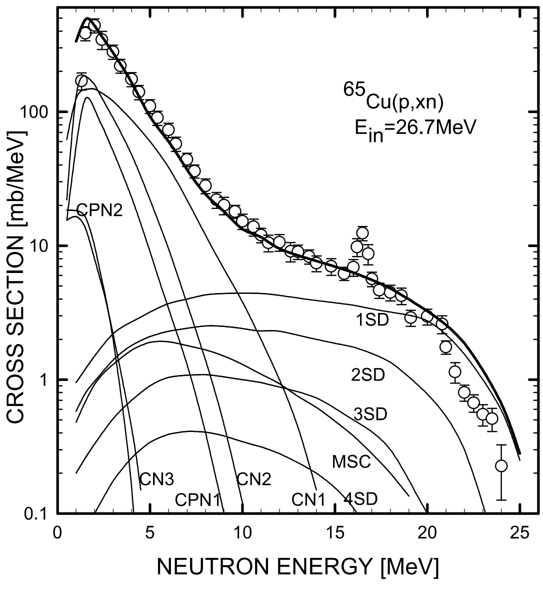

Fig. 6. Comparison of the MSD cross sections calculated with the non-DWBA matrix elements with the inclusive spectrum of neutrons emitted from the ^{65}Cu(p,xn)^{65}Zn reaction at incident energy of 26.7 MeV [18]. Labels CN1, CN2, CN3 show the primary, secondary and tertiary neutrons from the compound nucleus. CPN denotes neutron preceded by evaporation of a proton.

means that no single sequence is able to describe the corresponding MSD cross section for proton scattering satisfactorily. The same holds for the charge-exchange (p,n) reaction, although in this case the two strongest sequences, namely the (pnS^{-2},nn) and (ppS^{-2},pn)

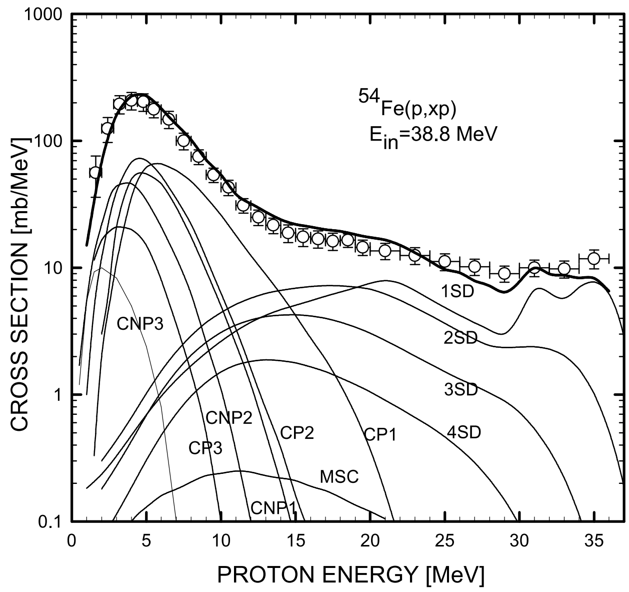

Fig. 7. Comparison of the MSD cross sections calculated with the non-DWBA matrix elements with the inclusive spectrum of protons emitted from the ^{54}Fe(p,xp)^{54}Fe reaction at incident energy of 38.8 MeV [19]. Labels CP1, CP2, CP3 are the primary, secondary and tertiary protons from the compound nucleus. CNP denotes proton preceded by evaporation of a neutron.

for 2SD, (pnS^{-2},nnS^{-2},nn) and (ppS^{-2},pnS^{-2},nn) for 3SD, etc., provide more than 90% of the corresponding MSD cross section, while the remaining sequences are negligible.

On the whole, the results show substantial contributions from MSD processes. These MSD cross sections together with the compound nucleus cross sections describe the measured inclusive nucleon emission spectra of ^{93}Nb(n,xn)^{93}Nb reaction, at incident energy of 25.7 MeV [17], ^{65}Cu(p,xn)^{65}Zn reaction, at 26.7 MeV [18] and ^{54}Fe(p,xp)^{54}Fe reaction, at 38.8 MeV [19], very well. This is shown in Figs. 5 to 7.

It is worth emphasizing that the calculation of the MSD cross sections for a given reaction requires the calculation of 1SD cross sections for all remaining reaction channels as well. This implies that, e.g. in a charge-exchange reaction the strong isoscalar modes are excited in parallel with the weaker isovector ones via the nucleon scattering stages in the multistep sequences.

3 Conclusions

We have used the enhanced non-DWBA matrix elements to describe consistently different nucleon induced reactions. Significant contributions from 1SD to 4SD reactions are obtained at incident energies below 40 MeV. On the other hand, normal DWBA, advocated by Feshbach [2,3], provides much smaller MSD cross sections. It seems that cross sections calculated in the framework of the RPA approach [20] when extended up to at least 3SD reactions could shed more light on the above controversy.

References

[1] H. Feshbach, A. Kerman, S. Koonin, Ann. Phys. (N.Y.) 125 (1980) 429.

[2] H. Feshbach, Ann. Phys. (N.Y.) 159 (1985) 150.

[3] H. Feshbach, Phys. Rev. C 48 (1994) R2253.

[4] T. Tamura, T.Udagawa, H. Lenske, Phys. Rev. C 26 (1982) 379.

[5] A. Marcinkowski, B. Mariański, Phys. Lett. B 433 (1998) 223.

[6] A. Marcinkowski, B. Mariański, Nucl. Phys. A 653 (1999) 3.

[7] P. Demetriou, A. Marcinkowski, B. Mariański, Phys. Lett. B 493 (2000) 281.

[8] A. Marcinkowski, P. Demetriou, B. Mariański, Nucl. Phys. A 694 (2002) 312.

[9] P. Demetriou, A. Marcinkowski, B. Mariański, Nucl. Phys. A 697 (2002) 171; Nucl. Phys. A 707 (2002) 354.

[10] A.J. Koning, M.B. Chadwick, Phys. Rev. C 56 (1997) 970.

[11] A. Marcinkowski, R.W. Finlay, J. Rapaport, P.E. Hodgson, M.B. Chadwick, Nucl. Phys. A 501 (1989) 1.

[12] M.S. Hussein, R. Bonetti, Phys. Lett. B 112 (1982) 189.

[13] I. Kumabe, M.Haruta, M. Hyakutake, M. Matoba, Phys. Lett. B 140 (1984) 272.

[14] S.M. Austin, in: eds. C.D. Goodman *et al*, *Proc. Conf. on (p,n) Reactions and the Nucleon-Nucleon Force*, Telluride, Colorado 1979 (Plenum Press, NY 1980) p. 203.

[15] E. Gadioli, P.E. Hodgson, Pre-Equilibrium Nuclear Reactions, Clarendon, Oxford, 1992, p. 385.

[16] A. Marcinkowski, P. Demetriou, Acta Phys. Pol. B, *to be published*.

[17] A. Marcinkowski, R.W. Finlay, G. Randers-Pehrson, C. Brient, R. Kurup, S. Mellema, A. Meigooni, R. Tailor, Nucl. Sci. Eng. 83 (1983) 13.

[18] E. Mordhorst, M. Trabandt, A. Kaminsky, H. Krause, W. Scobel, R. Bonetti, F. Crespi, Phys. Rev. C 34 (1986) 103.

[19] F.E. Bertrandt, R.W. Peelle, Phys. Rev. C 8 (1973) 1045.

[20] H. Lenske, H.H. Wolter, M. Herman, G. Reffo, *in* Proc. 7-th Int. Conf. on Nuclear Reactionn Mechanisms, Varenna, 1994, ed. E. Gadioli (Ric. Sci. Suppl. 100, 1994) p. 110.